Project 4: Modelling Phase Transitions in Magnetic Systems

Hedvig Borgen Reiersrud, Kamilla Ida Julie Sulebakk and Andrea Jensen Marthinussen
(Dated: November 30, 2020)

In this project we have utilized the Ising model in two dimensions in order to study phase transitions in magnetic systems. Using the Metropolis algorithm, we have calculated the expectation values of energy, magnetization, and their connected specific heat and magnetic susceptibility for systems with different lattice sizes and temperatures. Using a total number of Monte Carlo cycles equal to 10^4 we found that for a 2×2 lattice system with $T = 1.0$ J the analytically predicted and numerically calculated values for the observables comply to a great extent. When handling lattice size of 20×20 we observed that for a system with randomly ordered spin for $T = 1.0$ J and $T = 2.4$ J, the system reached equilibrium state after approximately 10^4 Monte Carlo cycles. For a system with ordered spin at $T = 1.0$ J, the system was in its equilibrium state already before sampling, as predicted. Additionally, we found that for a lattice size of 20×20 the obtained numerical critical temperature was 2.32 J, which was in 97.8 % compliance with the analytical value. Furthermore, when calculating the probability distribution, we found that for a low temperature, $T = 1$ J, almost all particles were in the same energy state. For $T = 2.4$ J we observed a large spread in energies, which is in alignment with our expectations. Furthermore, we have computed the numerical value of the critical temperature in the thermodynamic limit by increasing the lattice sizes. We found that in order to decrease the run-time, we would need to use parallelization which proved to be vastly beneficial. The obtained value of the critical temperature was $T_C = 2.25 \pm 0.05$. The analytical critical temperature was found to be within the standard deviation.

I. INTRODUCTION

Understanding the properties of a magnet is an essential part of physics. A magnetic field is generated when charged objects are accelerated or have the quantum mechanical feature called spin. As all elementary particles have spin, except from the Higgs boson, a material containing free elementary particles will generate a magnetic field. When a material generates a magnetic field as a result of its particles having spin, it is called a ferromagnet. The spin of the electrons in atoms is the main source of ferromagnetism. It is fascinating to simulate how the magnet generates magnetic fields and behave at different temperatures. The aim of this project is to simulate a phase transition of a magnetic material. The critical temperature is the temperature at which a material can coexist in two different phases, and for the most popular ferromagnets including the metals iron, cobalt and nickel it is generally very high. The critical temperature of a magnetic material has many interesting features, which we will investigate in this report.

The Ising model is a broadly used model. It can be used to simulate brain neurons, model motions of atoms in a gas and magnetism. Here we will focus on its ferromagnetic application, which initially was the motivation for the model. We will simulate a ferromagnet by assigning the particles with spin to points in a square lattice in to dimensions, where the particles can only interfere with their neighbouring lattice points. Though the model serve as a much simplified version of reality, as the system in actuality is enormously complicated, it can still provide us with valuable intuition for how ferromagnets behave close to the critical temperature. Through the Ising model we will analyze different observable quantities such as the energy and magnetic moment which affect the critical temperature.

In order to simulate the Ising model numerically we will use the Metropolis algorithm. The algorithm uses Monte Carlo cycles in order to simulate the estimations of the Ising model [4]. The algorithm initializes a matrix with the particles' spins ordered randomly to be either spin up or spin down. The simulation is stopped when a certain criteria is met. In this case, the result is a ferromagnetic structure where the spins are coordinated in the same direction. We will further analyze a probability distribution of the different energy states the system can be found to be in, which is a very exciting quantity to investigate. The algorithm can also be used in other to solve other cases, as is preforms a numerical integration which is applicable in many situations.

Because the lattice spins are randomly initialized in the Ising model, the energy and magnetization of the system will also be random, as both quantities are dependent of the spins. It will therefore prove necessary to utilize a random number generator in order to initialize the lattice. A computer cannot provide non-deterministic random numbers, although this is of little significance if the random number generator has a sufficient period length. In this project we will use the Mersenne Twister random number generator, which is by far the most used randomizer in computer science due to its large period length.

II. THEORY

The Ising model

The Ising model is a model describing ferromagnets in statistical physics. The model includes a discrete representation of the energy as well as the magnetization, the so-called magnetic dipole moment, of atomic spins. Magnetization reflects the total strength of a magnet. The discretization of the energy and the magnetization in the Ising model greatly simplifies the process we wish to describe numerically.

The quantum mechanical feature of spin is commonly represented by either spin pointing up, $\uparrow = 1$, or spin pointing down, $\downarrow = -1$. The spins involved in this simulation are positioned in a lattice, in which each particle is allowed to interfere with its neighbouring particles only. In reality, each particle with spin will generate its own magnetic field, thus, modelling a phase transition is a very complicated process for materials consisting of many moles of particles. Though the model is not thoroughly accurate, it will still give us valuable information of important physical properties of the system such as the critical temperature.

With no external magnetic field, the energy in the simplest form of the Ising model from ref. [1] is,

$$E = -J \sum_{\langle k,l \rangle}^{N} s_k s_l. \tag{1}$$

Where $\langle k, l \rangle$ demonstrates that we will only sum over nearest neighbouring particles. s_k and s_l have the value ± 1, and represents the spins of the lattice points k and l. N denotes the total number of lattice points. J is the coupling constant, signifying the strength of the interaction between neighbouring spins. Since J is only a constant, we can calculate the energy with the coupling constant as a unit. J varies for different materials. Since we ignore the value of J, our simulations are applicable to any magnetized material.

The magnetization, M, is the sum of each particle's spin. Therefore,

$$M = |\sum_{i}^{N} s_i|, \tag{2}$$

where s_i the spin of the lattice point i. In figure 1 two 2-d lattices are presented with different spins. From equation 2 the aligned spins have a higher magnitude of magnetization.

Statistical mechanics

The partition function is a dimensionless value describing the statistical assets of a system at equilibrium. That is, the system will not have a net flow of matter or energy, which results in the temperature being uniform. The partition function reads,

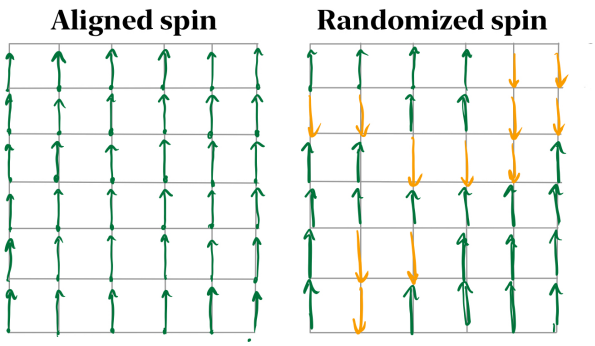

Figure 1. A schematic of a two dimensional lattice structure $L \times L$ where the lattice points' spins are aligned and randomized. The absolute value of the magnetization and energy is higher for the aligned spins.

$$Z = \sum_{i}^{N} e^{-\beta E_i}. \tag{3}$$

β is a constant equal to $\frac{1}{k_B T}$, where k_B is the Boltzmann's constant and T the temperature. E_i is the energy state of each of the $i \in \{1, N\}$ (in steps of 1) accessible states. $e^{-\beta E_i}$ is the so-called Boltzmann factor.

The partition function plays the role of normalizing the probabilities of observing a state i. The probability is,

$$P_i = \frac{1}{Z} e^{-\beta E_i}. \tag{4}$$

It is apparent that it is most likely to observe the lowest energy states. The relationship between probabilities of measuringn the energy states E_i and E_j is,

$$\frac{P_i}{P_j} = e^{(E_i - E_j)\beta}. \tag{5}$$

From equation 1, the change of energies, $\Delta E_{i,j} = E_i - E_j$, can be written as,

$$\Delta E_{i,j} = 2S_{i,j}(S_{i+1,j} + S_{i-1,j} + S_{i,j+1} + S_{i,j-1}), \tag{6}$$

when ignoring the coupling constant J.

Furthermore, we can use the partition function in order to find expressions of the expectation values of obtaining different physical properties, such as the magnetization $\langle M \rangle$ and energy $\langle E \rangle$.

$$\langle M \rangle = \frac{1}{Z} \sum_{i}^{N} M_i e^{-\beta E_i} \tag{7}$$

$$\langle E\rangle = \frac{1}{Z}\sum_{i}^{N} E_i e^{-\beta E_i} \tag{8}$$

Additionally, we can express the expectation values of the squared magnetization and energy in the same way. This let us calculate the standard deviation of the energies and magnetization. The heat capacity at constant volume, C_V, is proportional to the squared standard deviation of energy, σ_E. It reads,

$$C_V = \frac{\beta}{T}(\langle E^2\rangle - \langle E\rangle^2) = \frac{\beta}{T}\sigma_E^2. \tag{9}$$

The size proportional to the squared standard deviation of magnetization, σ_M, is the magnetic susceptibility, χ.

$$\chi = \beta(\langle M^2\rangle - \langle M\rangle^2) = \beta\sigma_M^2. \tag{10}$$

Phase transitions

The critical temperature, T_C, is defined as the temperature in which a system can be right between two states, e.g solid and liquid state. The critical temperature is therefore the temperature where the phase transition will appear. At T_C, the system is unstable, meaning a small change of spins, will result in a large change of the system, as the system is no longer right between two states. From figure 2, the different oriented flips are shown as black and white respectively. For increasing temperature, the model becomes more and more disordered. Therefore the highest rate of change of the observables will be at T_C.

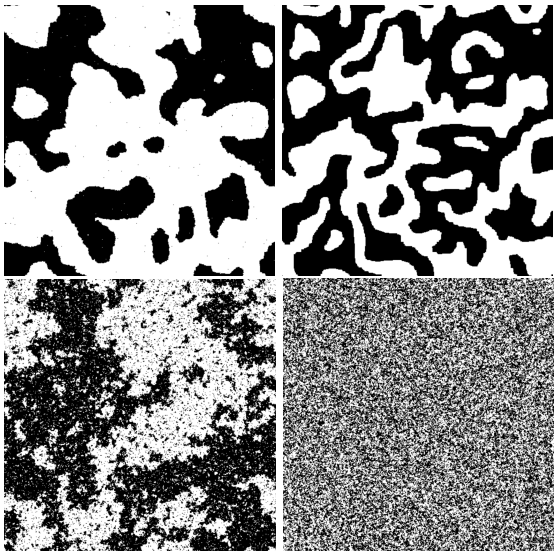

Figure 2. The figure displays a 512x512 Ising lattice, for $T = 0.0, T = 1.0, T = 2.269$ and $T = 4.0$ respectively. Up and down spins are white and black pixels. Ref. [5].

From ref. [1] we the following equation,

$$T_C(L) - T_C(L\to\infty) = aL^{-1/\nu}. \tag{11}$$

Where a is a constant. $T_C(L)$ is here a set of approximated critical temperatures for different values of L. Using this equation, we can arrive at $T_C(L\to\infty)$ which is the critical temperature near the thermodynamic limit.

When the temperature is near the critical temperature the system will have a higher temperature will have more accessible states. Thus the probability distribution in equation 4 will have a higher variance than for lower temperatures.

Analytic results

Lars Onsager was the first to solve the Ising model analytically in two dimensions. From ref. [1] Onsager's analytical solution of the critical temperature is presented. It states,

$$\frac{k_B T_C}{J} = \frac{2}{\ln(1+\sqrt{2})} \approx 2.269. \tag{12}$$

The analytical value is obtain when setting ν equal to 1. From figure 2 and ref.[5], it is apparent that the spin become disordered at $T = 2.269 \approx T_C$. For temperatures higher than T_C, the spin configuration become more and more chaotic.

Moreover, by using equations 3, 7 and 8, in addition to using the same method to find the expectation values of the squared magnetization and energy, we arrive at the analytical results which are deviated in Appendix A. They read,

$$Z = 12 + 4\cosh(8\mathrm{J}\beta), \tag{13}$$

$$\langle E\rangle = -8J\frac{\sinh(8J\beta)}{3+\cosh(8J\beta)} \tag{14}$$

$$\langle M\rangle = 2\frac{2+e^{8J\beta}}{3+\cosh(8J\beta)} \tag{15}$$

$$\langle E^2\rangle = 64J^2\frac{\cos 8J\beta}{3+\cosh(8J\beta)} \tag{16}$$

$$\langle M^2\rangle = 8\frac{1+e^{8J\beta}}{3+\cosh(8J\beta)} \tag{17}$$

The analytical values of heat capacity and susceptibility are easily obtained by equations 9 and 10. These are also deviated analytically in the appendix.

These results are for the lattice size of 2×2 with periodic boundary conditions (PBCs). PBCs are a set of boundary conditions which will generate a system which approximates for an infinite boundary condition. In equation 11 one would need to calculate for $T_C(L = \infty)$. It goes without saying that a computer cannot represent infinity, so we will approximate the infinite value with the PBCs.

III. ALGORITHM

The Metropolis algorithm

In this project we will use the Metropolis algorithm in order to simulate the Ising model to achieve numerical values of the different physical entities. Intuitively we would assume that in order to find the probability distribution for observing a system to be in a certain energy state, one would need to utilize the partition function in equation 3. However, this is a very costly computational operation, as one would need to iterate over every possible state. Instead we will use an algorithm which uses repeated random sampling in order to obtain numerical results of the probability distributions. The algorithm uses only ratios between probabilities, such that the partition function and the probability function in equations 3 and 4 are irrelevant to obtain the approximation of the probability distribution.

For this specific case, the algorithm reads;

Define number of sampling points N
Define matrix size $L \times L$
Randomize values of $s_{i,j}$ *for the* i, j *element in the matrix, 1 or -1*
Set $\langle E\rangle, \langle E^2\rangle, \langle M\rangle, \langle M^2\rangle = 0$
for $n \in \{1, N\}$ **do**
  for $l \in \{1, L^2\}$ **do**
    i, j randomly chosen in $\{1, L\}$
    r randomly chosen in $\{0, 1\}$
    if $\Delta E < 0$ **then**
      $s_{i,j} = -s_{i,j}$
      $E = E + \Delta E$
      $M = M + 2s_{i,j}$
    end if
    if $r < e^{-\beta \Delta E}$ **then**
      $s_{i,j} = -s_{i,j}$
      $E = E + \Delta E$
      $M = M + 2s_{i,j}$
    end if
  end for
  $\sum E = \sum E + E$
  $\sum E^2 = \sum E^2 + E^2$
  $\sum |M| = \sum |M| + |M|$
  $\sum M^2 = \sum M^2 + M^2$
end for
$\langle E\rangle = \sum E/N$
$\langle E^2\rangle = \sum E^2/N$
$\langle M\rangle = \sum |M|/N$
$\langle M^2\rangle = \sum M^2/N$

The Metropolis implementation of our algorithm chooses which spins to flip in a randomized matter, only allowing a spin in the lattice to change sign if the change in energy ΔE is negative, or at the occasional chance that a random number r between 0 and 1 is smaller than $e^{-\beta \Delta E}$. Performing this L^2 times per Monte Carlo cycle before updating the sums of the observables, the expectation values for the observables of interest is calculated ref[4]. Computers cannot truly choose a randomized number, through a random number generator (RNG). The randomized number is called a random seed state. Though seeming random, the randomized numbers are in actuality deterministic when given an initial random seed. In our program we will use the Mersenne Twister random number generator. The RNG has a period of $2^{1997} - 1$, meaning the RNG is *random* for programs which generate random numbers for a lower period than than $2^{1997} - 1$. The maximum matrix size we will simulate for is $L \times L = 100 \times 100$ with a number of 10^6 MCCs. This results in a period of 10^{10}. Since the Mersenne RNG is $\gg 5 \cdot 10^{10}$, it will be more than sufficient to randomize the spins and indices i and j for our largest number of sampling points and matrix size.

IV. METHOD

Initial spin	Final spin	Initial E	Final E	ΔE
$\uparrow$ $\uparrow\ \uparrow\ \uparrow$ $\uparrow$	$\uparrow$ $\uparrow\ \downarrow\ \uparrow$ $\uparrow$	-4J	4J	8J
$\downarrow$ $\uparrow\ \uparrow\ \uparrow$ $\uparrow$	$\downarrow$ $\uparrow\ \downarrow\ \uparrow$ $\uparrow$	-2J	2J	4J
$\downarrow$ $\downarrow\ \uparrow\ \uparrow$ $\uparrow$	$\downarrow$ $\downarrow\ \downarrow\ \uparrow$ $\uparrow$	0J	0J	0J
$\downarrow$ $\downarrow\ \uparrow\ \downarrow$ $\uparrow$	$\downarrow$ $\downarrow\ \downarrow\ \downarrow$ $\uparrow$	2J	-2J	-4J
$\downarrow$ $\downarrow\ \uparrow\ \downarrow$ $\downarrow$	$\downarrow$ $\downarrow\ \downarrow\ \downarrow$ $\downarrow$	4J	-4J	-8J

Table I. The table displays the different spin combinations of a lattice point and its neighbours in a initial state, i.e. before a possible flip of spin, and final state, after the flip of spin. The change of spins are calculated through equation 6. There are only 5 unique ΔEs possible for a two dimensional system.

Testing with theory

We start by initializing the lattice and write a code implementing the general Metropolis algorithm for the lattice size of 2×2 at temperature $T = 1$ J. The analytical values of the expectation values, from equations 14, 15, 16, and 17, can then be tested against the numerically obtained ones. If they match up, we can assume that the algorithm holds for a higher number of lattice points.

By using equation 12 we can compare our numerical result of the critical temperature to the analytical value. We expect that an increasing lattice size will generate critical temperatures which will become more and more coordinated with the analytical results.

Initial state

The two dimensional lattice structure containing $L \times L$ spins is initialized either as an highly ordered matrix where all spins are "up" or as a matrix where each spin is randomly chosen to be either "up" or "down" (1 or -1) by the Mersenne Twister RNG. Thereafter, the total energy of the system is calculated by 1, while the total magnetization of the system is calculated by 2.

For a system with all spins oriented as "up" and $T = 1$ J, we expect the system to be in its equilibrium state 5 from the initialization, thus we do not expect it to change after N MCCs. For higher temperatures T, the system will appear more and more chaotic. This is due to the fact that the most probable state of the system will then be that of particles being in different energy states. We do therefore expect the initially highly ordered system to change to a more "chaotic" configuration as we cycle through the Monte Carlo simulation.

Boundary conditions

Nonetheless, as we intend to simulate an infinite two dimensional grid, all lattice points need to have four neighbours. As the size of the matrix configuration must be finite, this is not realistically the case. The highest lattice size we will simulate is 100×100. However, by defining an indexing array simulating the PBCs as follows,

$$I = [L-1, 0, 1, ..., L-1, 0],$$

the problem for the outer-most elements only having two neighbours is avoided. In the loops where matrix elements are utilized, instead of indexing the matrix itself, by the indices i and j, we send the iterative index to the indexing array and use the indexing array as the index argument for the matrix. (skrive bedre)

In reality, a lattice size of 100×100 is minor compared to 'normal' magnets containing many moles (10^{23}) of particles. This is not solvable numerically, as one would need to loop over $> 10^{23}$ states. However, by using the boundary conditions above, one would expect to approximate a larger system.

Efficiency

The efficiency increases when we utilize the benefit of the Metropolis algorithm. That is the fact that we never have to calculate the partition function, only the energy differences, ΔE.

All the spins are either represented as $+1$ or -1, with ΔE given by equation 6, the only ΔE's possible for a two dimensional Ising model is shown in table I. As a result, the accessible change of energy states are $\Delta E = -8\text{J}, -4\text{J}, 0\text{J}, 4\text{J}, 8\text{J}$. Thus, it is irrelevant to calculate equation 6 for each value of the spins for j and i. By using only these 5 possible ΔEs will increase the efficiently to a great extent as the values can be calculated outside the loop to decrease the number of FLOPs (ref. [2]). As a consequence, we only need to calculate the five achievable change of energies. This will decrease the run-time substantially.

Additionally, we can avoid calling the exponential function L^2 times in the MCCs in order to calculate the probability distribution. This by only calculating for ΔE inside the cycle. After the MCC have accepted L^2 states, we can then go on and taking the result of ΔE as the exponent in order to obtain the probability distribution.

Equilibrium

When we initialize the lattice for the majority of this project, each lattice point is assigned a spin randomly. This initial configuration will likely not be an equilibrium state, and we thereby expect the system to approach equilibrium as the number of MCCs increase. We say that the system has reached equilibrium when the energy becomes constant in time. When the system has reached equilibrium, the number of MCCs is called the Burn-In period.

Units

We want to scale the temperature in such a way that the axis of the plots of quantities which depend on T are easily readable. We achieve this by setting the Boltzmann constant $k_B = 1$ and thus measuring T in units of energy. In addition to making the plots becoming more readable, scaling the quantities appropriately also helps us avoid under- and overflow.

Furthermore, the coupling constant J is generally quite large, and vary for different materials. To minimize numerical error, we will also set this constant to 1Joule [J]. This also let us generalize the simulation to different materials.

Numerical values of the critical temperature

In order to discuss the reliability of our results, we will compare the numerically obtained values of the critical temperature for different lattice sizes with the analytical T_C in equation 12.

We can obtain numerical values of the critical temperature in a myriad of different approaches. Here we will both use equation 11 and by using the traits of the phase transitions. We expect the spin configuration to be unstable near T_C, meaning the highest slope rate, will be at T_C when the number of flipped spins are plotted as a function of temperature. Furthermore, we can approximate the critical temperature by using the properties of the susceptibility and heat capacity near T_C. From ref. [6], we expect the critical temperature to appear when $\chi(T)$ is at its maximum for a value of L. This is a greatly approximated approach, however we will use equation 11, in order to obtain a result of the numerical heat capacity at the thermodynamic limit. Ee will run for $L = 40, 60, 80$ and 100 and let $T \in \{2.0, 2.5\}$ with 50 steps, and $N = 10^6$. After having numerically obtained values of T_C with varying Ls, we can do a linear regression of equation 11. By substituting $1/L$ with the new variable x. This leads to,

$$T_C(L) = ax + T_C(L \to \infty). \tag{18}$$

Thus, by doing a linear regression of the equation above we will arrive at an approximated value of the intercept equal to $T_C(L \to \infty)$.
When utilizing least square fit, the best line through all the data points will be drawn in such a way that the sum of squared residuals $\sum_{i=1}^{N}(T_C(x)_i - (T_C(x=0) + ax))^2$ are minimized, ref. [7]. We will preform a least square regression by using the library SciPy in the programming language Python.

Parallelization

Though already having increased the efficiency of our code considerably, the numerical operations we intend to perform is still costly for the larger lattice sizes which we intend to simulate, such as $L^2 = 60 \times 60, 80 \times 80$ and 100×100 with number of sampling points $N = 10^6$, for 15 different temperatures each. Thus, it proves necessary to parallelize our computation in order to decrease the run-time. Parallelization enables the simulation to run parallel on different processors ref. [3].

In our case we will utilize OpenMP in order to parallelize our MCCs in the C++ program language. This we will assume increases the run-time substantially. To check this improvement of the run time we will perform a test run of a lattice of size $L = 20$ for 20 different temperatures with an unparallelized code to compare with a system of the same size run with the parallelized code.

Moreover, as the run time for such large lattice sizes for many temperatures is substantial even with a parallelized code, it will prove important that we know our parallelized algorithm works, to avoid unnecessary time usage of running a program which gives unsatisfactory results. We will therefore implement a test option in our code which runs the same parallelized algorithm for a temperature we are already familiar with and know what to expect from the expecation values of the observables.

As the value of MCCs and L will be large numbers, we find it necessary to store these as "long ints" instead of regular "ints". This way we will avoid a possible integer overflow, that tends to happen when an operation attempts to create a numeric value outside of the range that can be represented with a given number of digits. An overflow condition can compromise the program's reliability, and one should therefore take necessary precautions in order to avoid this.

V. RESULTS

The 2 × 2 lattice size

The figures in figure 3 and 4 display the analytical and numerical $\langle E\rangle, \langle M\rangle, C_V$ and χ as functions of temperature. It is apparent that the numerical value to a large degree matches the analytical value for all the physical quantities.

	Analytical	Numerical	Differences
$\langle E\rangle$	-1.99598	-1.99600	$2.00 \cdot 10^{-5}$
$\langle E^2\rangle$	3.99197	3.98200	$9.97 \cdot 10^{-3}$
$\langle\lvert M\rvert\rangle$	0.998661	0.998645	$1.60 \cdot 10^{-5}$
$\langle M^2\rangle$	0.99833	0.99832	$1.00 \cdot 10^{-5}$
χ	0.0010027	0.0010282	$8.01 \cdot 10^{-5}$
C_V	0.0080206	0.0079840	$3.66 \cdot 10^{-3}$

Table II. Table of analytically and numerically calculated expectation values and their corresponding χ and C_V, in addition to their differences. These values are for $N = 10^5$, lattice size 2×2 and temperature $T = 1$.

From table II it is shown that the differences of the analytical and numerical values vary. The highest difference, 10^{-3}, being for $\langle E^2\rangle$ and the lowest, 10^{-5}, for $\langle M^2\rangle$.

The figures in figure 5 display the analytical and numerical C_V and χ as functions of MCCs. The analytical values stay constant for different MCCs. The numerical values however, are not constant. Nevertheless the differences between the analytical and numerical susceptibility are quite low. However, after about $N = 10^4$ an

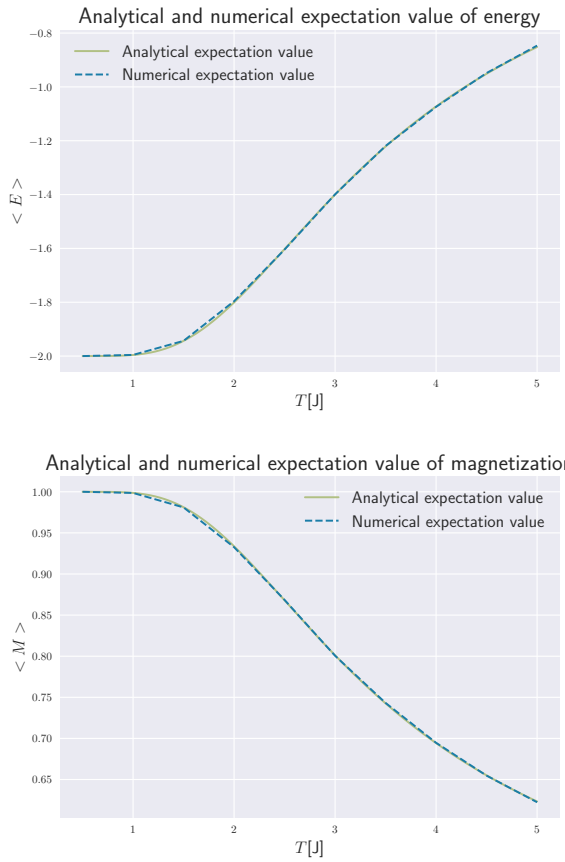

Figure 3. The figure shows the agreement between the numerical and analytical expectation energy and magnetization as functions of T for a 2×2 lattice with $N = 10000$.

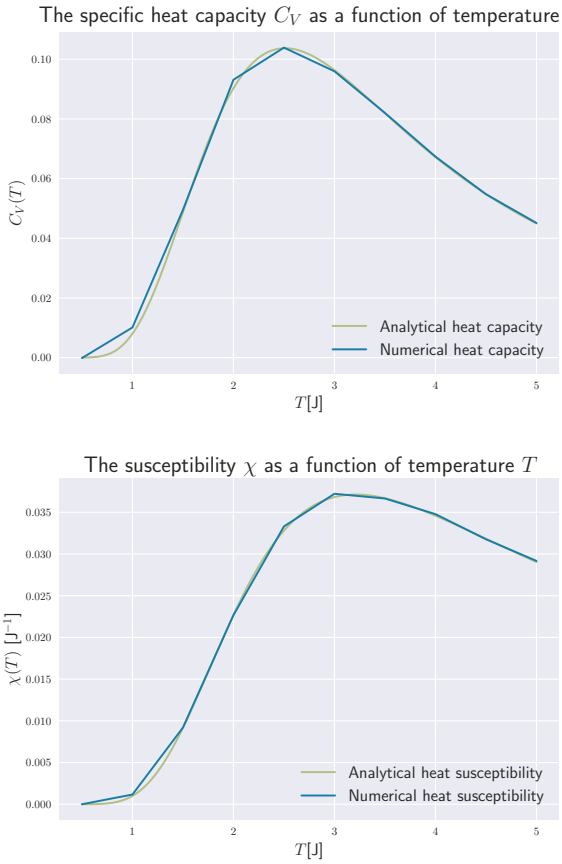

Figure 4. The figure shows the agreement between the numerical and analytical specific heat capacity and susceptibility as function of T for a 2×2 lattice with $N = 10{,}000$.

increasing number of MCCs does not seem to affect the compliance between the analytical and numerical values.

The 20 × 20 lattice size

From the figures in 6, the expectation values of the energy and magnetization as functions of MCCs is shown. The expectation values for both the magnetization and energy seem to be more and more constant for increased values of MCCs. In addition, the ordered spins at $T = 1$ and $T = 2.4$ are lower than the randomly initialized spins at the equal temperatures. For the magnetization the ordered spins for $T = 1$ and $T = 2.4$ are higher than the randomly initialized of spins. The ordered spins for $T = 1$ are constant for all N.

The figure 7 shows that the number of accepted flips for $T = 2.4$ have a higher slope rate than for $T = 1$. Additionally, the function of accepted flips appear to be linear. From the figure, it seems that the number of accepted spins for $T = 1$ stay constant at 0. However, looking closely at the figure, there is a slight increase in the number of flips for $T = 1$.

In figure 8, the number of accepted flips with temperatures varying from 0 to 5 is presented. The highest rate of change is obtained at ≈ 2.32, and represents the critical temperature. This is in 97.8 % compliance with the analytical value equal to 2.27.

Temperature	σ_E	${\sigma_E}^2$
1.0	$6.49 \cdot 10^{-3}$	$4.22 \cdot 10^{-05}$
2.4	$1.42 \cdot 10^{-1}$	$2.02 \cdot 10^{-2}$

Table III. The tables shows the standard deviation σ_E and variance σ_E^2 from the probability distribution of energy at $T = 1.0$ and $T = 2.4$.

The figures in 9 show the normalized probability of measuring different energies in the system. We see that for T = 2.4, close to the critical temperature, the probability takes a Gaussian distribution form. In comparison, for T = 1, the system seems to stabilize around -800 J.

Table III shows the variance and standard deviation of the two probability distributions. It is apparent that the standard deviation is must smaller for $T = 1$ than for $T = 2.4$.

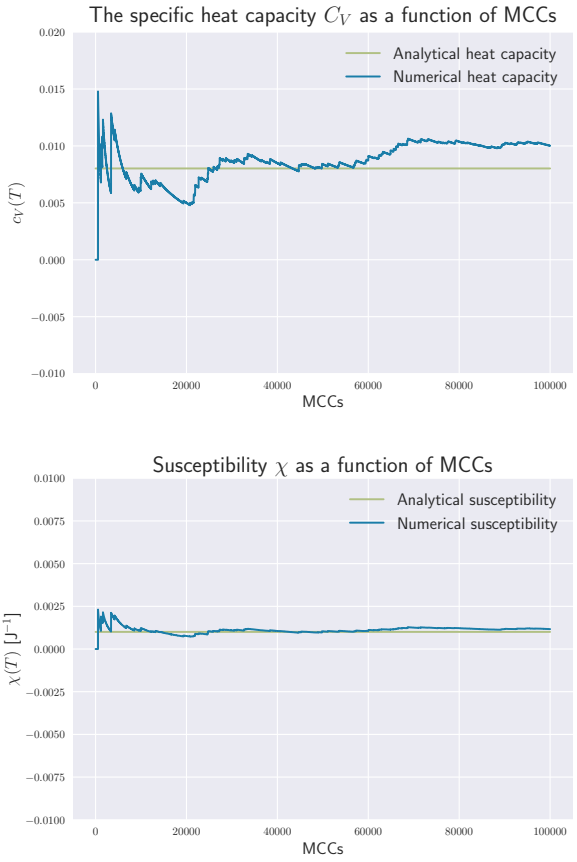

Figure 5. The figure shows the specific heat capacity and susceptibility for T = 1, as a function of number of MCCs compared with analytical value, for $L = 2$

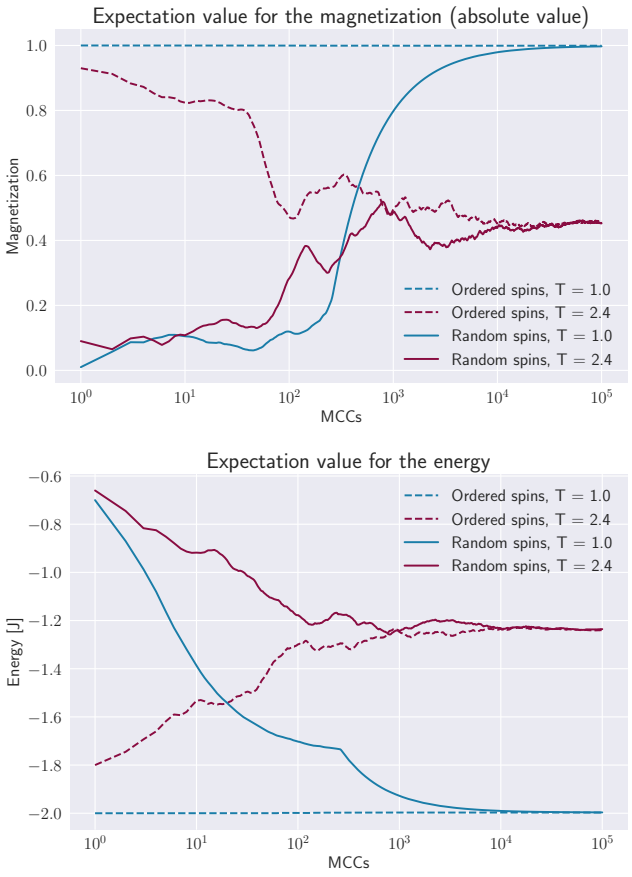

Figure 6. The figures display the expectation value of the magnetization and energy as function of MCCs.

Lattice size larger that 20 × 20

When parallelizing the simulations the run-time decreased substantially. The run-time without parallelizing our code for the lattice size 20×20 with $N = 10^6$ and 20 steps of temperature was 8.3 minutes. When parallelizing the code, we were able to run for the same values of L, N and temperature steps, the run-time was 2.0 minutes for 20 steps of temperature. Thus, the run-time decreased with 6.3 minutes when parallelizing.

L	Run-time [min]	Difference in run-time [min]
60	10.8	-
80	24.7	13.9
100	34.0	9.3

Table IV. The table displays the run-times for varying lattice sizes, and the differences between the previous and current run-times. The run-times were for MCCs $= 10^6$ and 15 steps of temperature in the interval $T \in [2.20, 2.35]$.

From table IV, we see that the run-times increase with the lattice sizes, when we have parallelized our code. The differences do not seem to have a specific pattern. We also found that the run-times vary with ±2 minutes each time we run the code.

The figures in 10 show how the magnetic susceptibility as function of temperature varies for different lattice sizes. We can observe that the data points form an arrow in the case for $L = 80$ and $L = 100$. However, for $L = 60$, the data points seem chaotically ordered.

We include a graphical representation of the susceptibility as function of temperature for $L = 40$ 11, as this was one of the other lattice sizes we were supposed to simulate. The reason for only plotting for $L = 60, 80$ and 100 in 10 was due to inconsistent results for lower sizes of lattices for various temperature intervals when trying to do this part of the project.

The figures in 12 display the magnetic susceptibility χ as function of temperature. The figures show how the quantities varies for different sizes of L. It is again observed that something is quite off in the case of $L = 60$, referring to the sudden spikes in the graph.

In figure 13 we see the linear regression of equation 18. The value of the intercept is equal to the critical temperature for $L \to \infty$. Estimated $T_C(L =\to \infty) = 2.25$, with a standard error of 0.05.

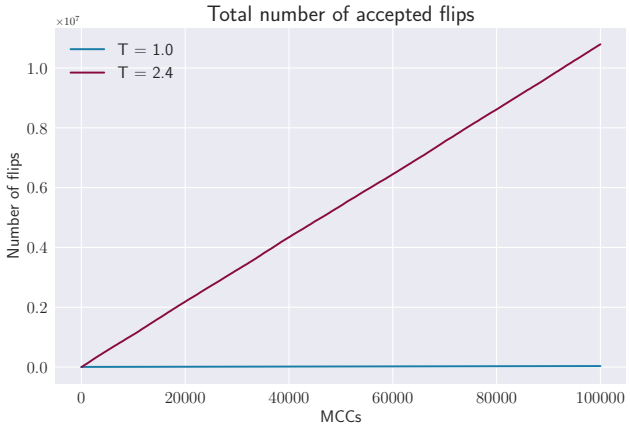

Figure 7. The figure displays the number of accepted flips of spin elements of the lattice as function of Monte Carlo cycles for $T = 1.0$ and $T = 2.4$.

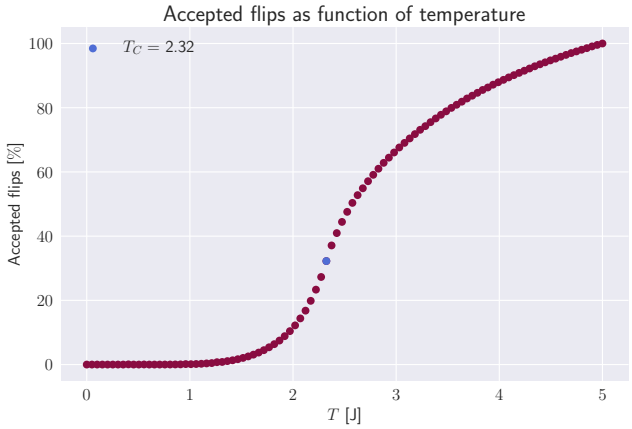

Figure 8. The figure displays the number of accepted flips of spin elements of the lattice as function of temperature. We see that at $T \approx 2.32$, the graph has the highest rate of change. This is for $L^2 = 20 \times 20$ and MCCs = 100,000.

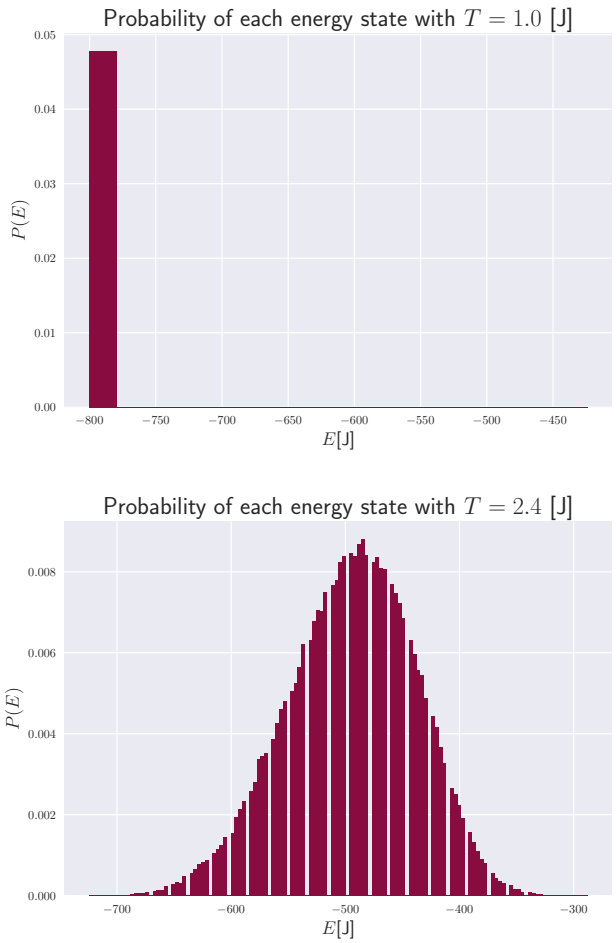

Figure 9. The figures display the normalized probability $P(E)$ for L = 20 with $T = 1$ and $T = 2.4$.

VI. DISCUSSION

The 2 × 2 lattice size

The agreement between the numerical and analytical values of the expectation values and their connecting χ and C_V are quite satisfying as shown in the figures in 3 and 4. As the agreement seems to hold for all temperatures, it is safe to say that these tests have succeeded and that our algorithm will hold for a larger number of lattice size.

L	$T_C(L)$
60	2.308
80	2.292
100	2.276

Table V. The table displays the different values of $T_C(L)$ for varying lattice sizes estimated from the magnetic susceptibility.

In the figures in 5, the compliance between the analytical value and the numerically computed values $\chi(T)$ and $C_V(T)$ as functions of number of MCCs seems, as expected, to become better and better for a higher number of MCCs. The intervals along the vertical axis are small, which indicates that the differences between the analytical and numerical heat capacity and susceptibility are inconsequential. The small differences we can observe in the figures might be due to small numerical errors. As they are remarkably small, they will however, most probably not affect larger calculations to a great extent. In other words, when testing the numerically calculated observables against the analytical for $L \times L = 2 \times 2$, we observe that they to a large degree match up. Again, we can therefore assume that the tests have succeeded in producing numerical results complying with the analytically expected ones.

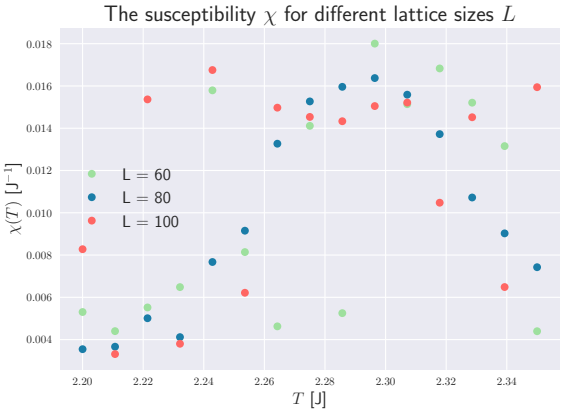

Figure 10. The figures display magnetic susceptibility per spin as function of temperature for $L = 60, 80 and 100$.

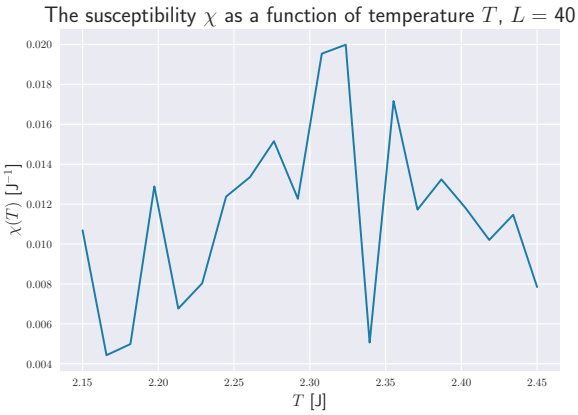

Figure 11. The figures display the magnetic susceptibility χ as function of temperature for $L = 40$.

From table II, we observe that the numerical values of the different physical entities are to a high extent complying with the analytical values in the case of the number of MCCs $= 100,000$ and $L = 2$. Once more, this indicates that the algorithm produces results with a high level of precision.

The 20 × 20 lattice size

Figures 6 show the expectation value of energy and magnetic moment for ordered and random spin orientation with $T = 1$ and $T = 2.4$. It is apparent that the system reaches an equilibrium situation for both temperatures at MCCs $\approx 10^4$. Moreover, we see from figure 7 that we have a more chaotic state for T = 2.4, as the number of accepted spin flips increases with increasing MCCs. In other words the number of accepted flips increases with increasing temperature, T, indicating that the system gets more and more disordered.

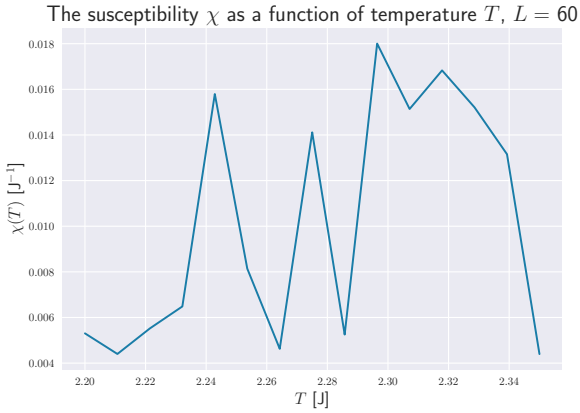

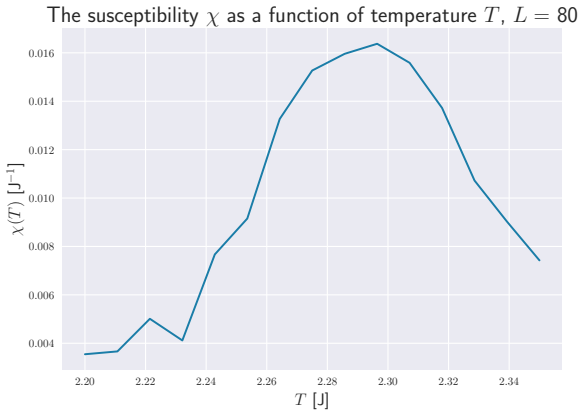

Figure 12. The figures display the magnetic susceptibility χ as function of temperature for two different sizes of L.

If one were to assume that the slope rate at its maximum at the critical temperature in figure 8, we obtained the value numerical value $T_C \approx 2.32$. Thus we receive a quite large difference between the numerical and analytical value in equation 12. This difference may be due to numerical errors, and could have been avoided with a higher number of MCCs, by using a smaller step in temperatures or increasing the lattice size. Nonetheless, the obtained T_C indicates that our algorithm produces results with somewhat accurate precision, which is fulfilling.

In figure 7 the shape of the graph representing number of accepted configurations for $T = 1.0$ appears to be constant, however, this is presumably only because of the much higher number of accepted configurations for $T = 2.4$ and thus the too large choice of interval on the vertical axis as the system is more chaotic. If we had plotted the two graphs by themselves they would both be observed to be linearly growing.

We arrive at the probability distributions for $T = 1$ and $T = 2.4$, without ever having to calculate it. The probability $P(E)$ for the 20×20 system for the two

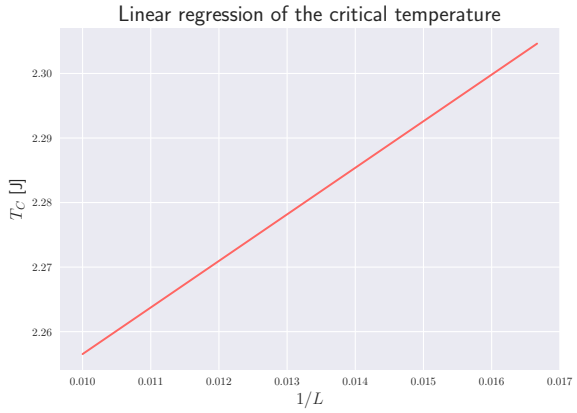

Figure 13. The figure display the linear regression of equation 18, where the intercept is the critical temperature in the thermodynamic limit.

temperatures, which are displayed in 9, have quite different shapes. For $T = 1.0$ the distribution function is very narrow compared to $T = 2.4$, which provides a large spread for the different energy values. It is evident that for a temperature under T_C, almost all energies occur at -800 J. For the temperature close to the critical, $T = 2.4$, the distribution takes an Gaussian form with mean -500 J. The Boltzmann distribution in equation 5 is proportional to a Gaussian distribution. This corresponds with theory, since equation 4 indicates that the lowest temperature level (the scaled $T = 1$) will be in the lowest energy state. For $T = 2.4$ however, the system is more chaotic, as the probability of flipping spins is high such that particles also may find themselves in the higher energy states.

We arrive at the standard deviation in energy σ_E equal to 0.006 and 0.14 for $T = 2.4$ and $T = 1.0$, respectively. Thus, the standard deviation of $T = 1$ is a a factor $\approx 1/10^2$ smaller than for $T = 2.4$. Since there are no analytical expression of the standard deviation for $L = 20$, we do not have anything to compare these values with. Even though the distribution is not completely Gaussian, the standard deviations say a lot about the shape of the probability distribution.

Lattice size larger that 20 × 20

In the last part of this project we wanted to study the behavior of the Ising model in two dimensions close to the critical temperature as function of the lattice size $L \times L$. When calculating the expectation values for E, M, E^2 and M^2, in addition to C_V and χ as function of $T \in \{2.20, 2.35\}$, we parallelized our code with OpenMP. We chose L to be $40, 60, 80, 100$, along with a step in temperature $\Delta T = 0.01$. The parallelization proved to be very beneficial in order to decrease the run-time when running the Metropolis algorithm. This was apparent when running the non-parallelized and parallelized code for $L^2 = 20 \times 20$ with MCCs $= 10^6$ and 15 temperature steps. The decrease of run-time between the non-parallelized code and the parallelized code was found to be 6.3 minutes for a lattice of this size, which is an enormous improvement and showed the huge impact parallelization had in our case.

We assume that the approximated numerically obtained values of T_C appear at the maximum value of $\chi(T)$ and C_V in figure 12. These values we have named $T_C(L)$, and their values are displayed in V. The obtained values of T_C in table V are in somewhat agreement with what we should expect, as the difference between the numerical and analytical value of T_C decreases with increasing MCCs. However, for $L = 40$, the difference between the numerical and analytical value of T_C was quite distressing. Therefore, we will only include the values of $T_C(L)$ for $L = 60, 80$ and 100, when calculating the critical temperature near the thermodynamic limit. We found that $T_C(L \to \infty) = 2.26 \pm 0.05$. The analytical value seems to comply the numerical value with the error ± 0.05.

We have encountered many challenges in our computations in the programming language C++. The largest being the overflow when declearing the integrers, such as the number of MCCs, as integrer types. Therefore, we have been obliged to declaring the integers as floating points which take 8 bytes, resulting in consuming too much memory for our largest Ls. These number of MCCs, temperature steps and lattice points produce therefore mysterious results, which is apparent in the figures **??**. Thus, the produced results of the critical temperature near the thermodynamic limit may have many sources of error. However, we are unsure of the significance of the source of error. Therefore, we cannot conclude whether or not these result are viable.

VII. CONCLUSION

We have utilized the Ising model in two dimensions for different lattice sizes, $L \times L$, in order to study a phase transition. Together with the Metropolis algorithm, the Ising model has allowed us to calculate the expectation values of mean energy, the absolute value of the magnetization, the specific heat and the susceptibility as functions of temperature. We have found that the numerically calculated values to a large degree complied with the values analytically predicted. This agreement held for a number of Monte Carlo cycles larger than 10^4. Hence, we can assert that the algorithm will hold for a higher number of lattice sizes.

When increasing the lattice size to 20×20, we found that the number of Monte Carlo cycles needed in order to reach the most likely states were 10^4 for a randomly initialized spin orientation with $T = 1$ and

$T = 2.4$. Additionally, we have found that the ordered initialized spins for $T = 1$ are stable for all numbers of MCCs. Pleasingly, this acts in accordance to theory. Furthermore, when computing the probability $P(E)$ for the 20×20 lattice with $T = 2.4$, we found that the probability distribution of energy followed Gaussian form, as predicted. For a temperature under the critical, $T = 1$, almost all particles found themselves in the lowest energy state, with $E = -800J$. As a result, the variance in energy for $T = 2.4$ is to a high extent larger than the variance in energy for $T = 1$, which is what one would expect.

When running the metropolis algorithm for large numbers of Monte Carlo cycles and lattice sizes, along with a great number of steps in temperature, we utilized parallelization. This resulted in a sufficient decrease of runtimes, but when we utilized our results to try to decide the critical temperature we ran into a lot of trouble. We still managed to get somewhat okay results for lattices of sizes 60×60, 80×80, and 100×100, although the graphical representation showed to be quite chaotic. In the thermodynamic limit we did luckily find that the numerical critical temperature was in high compliance with the analytical value. The numerically obtained critical temperature was $T_C(L \to \infty) = 2.26 \pm 0.05$, and the analytical value is within the standard error.Even though having had issues with memory loss, the result do somewhat comply with the analytical value.

GITHUB

All data, code and plots are available at our GitHub page: https://github.com/hedvigborgen/fys3150. Follow the README.md file in order to run the codes.

REFERENCES

- [1] Project 4 - FYS3150 (2020), M. H. Jensen, https://github.com/CompPhysics/ComputationalPhysics/blob/master/doc/Projects/2020/Project4/pdf/Project4.pdf

- [2]Project 1 - Solving the one dimensional Poisson Equation (2020), K. Sulebakk, A. Marthinussen, H. Reiersrud. https://github.com/hedvigborgen/fys3150/blob/master/project1/FYS3150___Project_1.pdf

- [3] Parallel Algorithms (date unknown), G. E. Blelloch and B. M. Maggs, Carnegie Mellon University, https://www.cs.cmu.edu/~guyb/papers/BM04.pdf

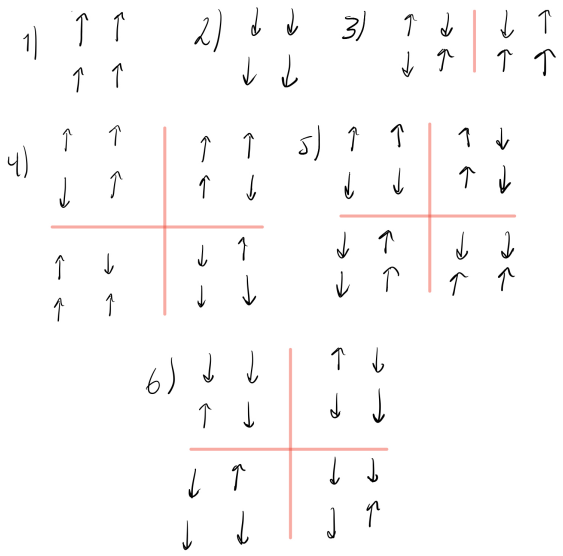

Figure 14. The spin configuration for a 2×2 lattice size. 1) and 2) have degeneracy 1, 3) two-fold degeneracy and 4), 5) and 6) have a four-fold degeneracy.

- [4] "Monte Carlo Methods in Statistical Physics"(1999), Newman M. E. J., Barkema G. T., Clarendon Press.

- [5] Ising lattice simulation (Oct. 2015) https://www.ibiblio.org/e-notes/Perc/ising.htm

- [6] The Analytical Expressions for a Finite-Size 2D Ising Model (date unknown), M.Yu. Malsagov, I.M. Karandashev and B.V. Kryzhanovsky, Russian Academy of Sciences https://arxiv.org/pdf/1706.02541.pdf

- [7] "Practical physics" (2001), G. L. Squires, Cambridge University Press, Page:29–52

VIII. ACKNOWLEDGEMENTS

Thanks to all the very helpful group teachers and Håkon Kvernmoen for investigating some very intricate problems in our code.

IX. APPENDIX

Deviation of the analytical results for the lattice size 2 × 2

In order to obtain the analytical results for 2×2 number of lattice points, we will use the configurations presented in figure 14. The magnetization and energies are obtained by equations 2 and 1. We start by using equation 3 in order to calculate the analytical value of the partition function. It reads,

$$\sum_i^{L\times L} e^{E_i\beta} = e^{8J\beta} + 4e^0 + 4e^0 + 4e^0 + 2e^{-8J\beta} + e^{8J\beta} = 12 + 2e^{8J\beta} + 2e^{-8J\beta} = 12 + 4\cosh(8J\beta).$$

For the expectation value of magnetization, we will use equations 2 and 7. It yields,

$$\langle M\rangle = \frac{1}{Z}\sum_i^{L\times L} M_i e^{E_i\beta} = \frac{1}{Z}(4e^{8J\beta} + 4\cdot 2e^0 + 4\cdot 2e^0 + 4e^{-8J\beta}) = \frac{16 + 4e^{8J\beta} + 4e^{8J\beta}}{12 + 4\cosh(8J\beta)} = 2\frac{2 + e^{8J\beta}}{3 + \cosh(8J\beta)}.$$

In addition, the expectation value for the squared magnetization is expressed in the same way as in equation 7 by substituting M_i with M_i^2. This results in,

$$\langle M^2\rangle = \sum_i^{L\times L} \frac{M_i^2 e^{-E_i\beta}}{Z} = \frac{1}{Z}(4^2 e^{8J\beta} + 4^2\cdot 2e^0 + 4^2 e^{-8J\beta}) = 8\frac{1 + e^{8J\beta}}{3 + \cosh(8J\beta)}.$$

We calculate the analytical expectation value of energy by equation 8.

$$\langle E\rangle = \sum_i^{L\times L} \frac{E_i e^{-E_i\beta}}{Z} = \frac{1}{Z}(-8\cdot 2e^{8J\beta} + 8\cdot 2e^{-8J\beta}) = -16J/4\frac{e^{8J} - e^{-8J}}{3 + \cosh(8J\beta)} = -8J\frac{\sinh(8J\beta)}{3 + \cosh(8J\beta)}.$$

We arrive at the squared expectation value of the energy in the same matter as for squared magnetization.

$$\langle E^2\rangle = \sum_i^{L\times L} \frac{E_i^2 e^{-E_i\beta}}{Z} = \frac{1}{Z}((-8)^2\cdot 2e^{8J\beta} + 8^2\cdot 2e^{-8J\beta}) = \frac{64J^2}{4}\frac{e^{8J} + e^{-8J}}{3 + \cosh(8J\beta)} = 64J^2\frac{\cosh 8J\beta}{3 + \cosh(8J\beta)}$$

As for the heat capacity C_V and susceptibility χ we use equations 9 and 10 and the results above to achieve the analytical results.

$$C_V = \frac{\beta}{T}(\langle E^2\rangle - \langle E\rangle^2) = \frac{\beta}{T}(64J^2\frac{\cosh(8J\beta)}{3 + \cosh(8J\beta)} - (-8J)^2(\frac{\sinh(8J\beta)}{3 + \cosh(8J\beta)})^2) = \frac{64J^2}{\beta}\frac{3\cosh(8J\beta) + \cosh^2(8J\beta) - \sinh(8J\beta)}{(3 + \cosh(8J\beta))^2} = \frac{64J^2}{\beta}\frac{3\cosh(8J\beta) + 1}{(3 + \cosh(8J\beta))^2}$$

$$\chi = \beta(\langle M^2\rangle - \langle M\rangle^2) = \beta\Big[8\frac{1 + e^{8J\beta}}{3 + \cosh(8J\beta)} - \Big(2\frac{2 + e^{8J\beta}}{3 + \cosh(8J\beta)}\Big)^2\Big] = 4\beta\Big[\frac{2(1 + e^{8J\beta})(3 + \cosh(8J\beta)) - (2 + e^{8J\beta})^2}{(3 + \cosh(8J\beta))^2}\Big] = 4\beta\frac{3 + 2e^{8J\beta} + \cosh(8J\beta)}{(3 + \cosh(8J\beta))^2}$$